JCTC Journal of Chemical Theory and Computation

Article

pubs.acs.org/JCTC

State-Selective Excitation of Quantum Systems via Geometrical Optimization

Bo Y. Chang,[†] Seokmin Shin,[†] and Ignacio R. Sola*[,‡]

[†]School of Chemistry (BK21[+]), Seoul National University, Seoul 151-747, Republic of Korea

[‡]Departamento de Química Física, Universidad Complutense, 28040 Madrid, Spain

ABSTRACT: We lay out the foundations of a general method of quantum control via geometrical optimization. We apply the method to state-selective population transfer using ultrashort transform-limited pulses between manifolds of levels that may represent, e.g., state-selective transitions in molecules. Assuming that certain states can be prepared, we develop three implementations: (i) preoptimization, which implies engineering the initial state within the ground manifold or electronic state before the pulse is applied; (ii) postoptimization, which implies engineering the final state within the excited manifold or target electronic state, after the pulse; and (iii) double-time optimization, which uses both types of time-ordered manipulations. We apply the schemes to two important dynamical problems: To prepare arbitrary vibrational superposition states on the target electronic state and to select weakly coupled vibrational states. Whereas full population inversion between the electronic states only requires control at initial time in all of the ground vibrational levels, only very specific superposition states can be prepared with high fidelity by either pre- or postoptimization mechanisms. Full state-selective population inversion requires manipulating the vibrational coherences in the ground electronic state before the optical pulse is applied and in the excited electronic state afterward, but not during all times.

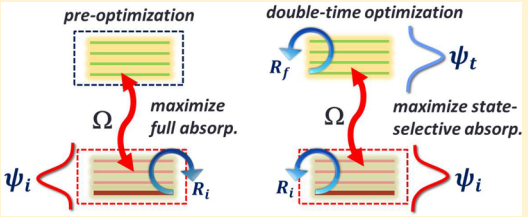

INTRODUCTION

The selective preparation of arbitrary states by means of laser protocols is a paramount goal of quantum control,[1−4] one that has primary importance in quantum engineering, particularly in quantum information, and quantum computation processes.[5] Quantum optimal control theory is especially well designed to find the optimal pulses.[6−9] There are general quantum controllability theorems that can be used to establish the feasibility of the control[3,10,11] while the study of the quantum landscapes can provide additional details regarding the topological features of the optimal solutions.[12−14]

A common quantum control problem can be recast as an optimization problem where one seeks to maximize the yield of some transition from the initial state $|\psi(0)\rangle$ to the desired "target" state $|\psi_t\rangle$, at time $t = T$, $|\langle\psi_t|U(T,0;\Omega(t))|\psi(0)\rangle|^2$, where the external pulse or Rabi frequency, $\Omega(t)$, is the time-dependent variational function and U is the time-evolution operator. The control function can be parametrized,[15−19] either to input experimental constraints or to constrain the search for the possible control mechanism.[20−23] Although the constraints may hinder the success of the optimization,[4] they are sometimes necessary to avoid unphysical solutions. For instance, the optimal pulses may use frequencies or intensities that induce phenomena not described by the Hamiltonian, as multiphoton or ionization processes, providing yields much larger than what would be realistically expected. At the very least, most optimal control algorithms use cost terms in the functionals that penalize solutions that involve large pulse intensities.[8,24,25]

In general, mapping the yields as a function of a few important parameters often provides a simplified landscape of the control that is useful to identify the robustness and key limits in the control of the dynamics.[26]

In this work we are interested in exploring generic features of the control of multilevel systems with manifolds of sublevels, what we call quantum structures. Most physical systems allow the labeling of approximate quantum numbers. A prototype case consists of separable systems where, at least under certain conditions, one clearly identifies subsystems that can be addressed independently of each other, as in quantum information systems.[5] However, practically all nonseparable complex systems show a hierarchic structure due to the different effective masses participating in the different motions. The hierarchical model allows one to describe the system in terms of manifolds with different sublevels, that can be addressed (at least to a certain approximation) independently. For instance, this is certainly the case in molecules, where the electronic, vibrational, and rotational degrees of motion are relatively decoupled and clustered, so that in many cases one can identify and independently address rotational levels within vibrational levels and vibrational levels ascribed to different electronic states. This particular Hamiltonian structure can be used to determine what physical resources are needed and how to apply them when controlling population transfer between different sets of states.

Received: June 4, 2015
Published: July 28, 2015

DOI: 10.1021/acs.jctc.5b00522
J. Chem. Theory Comput. 2015, 11, 4005−4010

In this regard, we have recently analyzed the key limiting physical properties in ultrafast electronic absorption by broadband transform-limited pulses. If one is not allowed to *shape* (modulate) the field, the excited vibrational levels in the ground potential induce Stark shifts that decouple the excited electronic state from the initial state, drastically reducing the yield of absorption. However, by preparing suitable superpositions of vibrational states before the field acts, that is, by engineering the initial wave packet, one can achieve maximal population transfer at the highest possible rate. The proposed scheme was named quantum control by parallel transfer.[27]

Interestingly, the method was found by a novel optimization process. Separating the treatment of the different degrees of freedom in the Hamiltonian and assuming certain constrained controllability, one can rewrite the control problem as an optimization of the initial wave function within a subset of vibrational eigenstates that are accessible at initial time. Then one can use the Rayleigh−Ritz variational method applied, not to minimize the energy as is usual in quantum chemistry,[28] but to maximize transition probabilities. This approach is equivalent to a geometrical optimization of the dynamics where the time-evolution operator is replaced by an ordinary rotation in a subset of the Hilbert space. Therefore, it must be applied *locally* on a certain structure of the Hamiltonian, and *locally* in time, so that the process is separated from the dynamical control exerted from the external field $\Omega(t)$.

The geometrical optimization (GO) is a very general tool. In this work we will generalize the procedure to perform optimization at an initial time within the ground state, so-called geometrical preoptimization, as well as within the excited state at a final time, or geometrical postoptimization. We will also allow both transformations, as in the double-time geometrical optimization. Although in principle GO can be used together with other control approaches that optimize certain pulses, for instance, the optical pulse that couples the ground and excited electronic states, in this work this pulse will be kept fixed as a control parameter. The different results of GO are then shown as a function of this parameter, in particular, of the pulse integral. We will apply these procedures to two important dynamical problems involving state-selective population transfer. The first is the preparation of specific superposition states with high fidelity that can be used to implement quantum information protocols in molecules.[29] The second is population inversion to weakly coupled excited states, a problem of interest in spectroscopy.

GEOMETRICAL OPTIMIZATION PROCEDURE

In this work we will focus on systems with two substructures identified by two quantum numbers $|a,n\rangle$: The first one has two possible values: g (for ground) and e (for excited), while $n \in [1,N_g]$ in the first manifold and $n \in [1,N_e]$ in the second. The procedure can be easily generalized for more quantum numbers or a larger set of values. Although we will study general Hamiltonians with few free parameters, we will often regard these substructures as corresponding to the electronic state and its corresponding vibrational levels.

As initially stated, we want to maximize at time T the transition probability to a certain state $|\psi_t\rangle = \sum_j b_j |e,j\rangle$ defined on the excited state manifold. We will constrain the search of $\Omega(t)$ factorizing $U(T,0;\Omega(t)) = U_i(T,t_f;\Omega_f)\ U_{ge}(t_f,t_i;\Omega_{ge})\ U_f(t_i,0;\Omega_i)$. Here $\Omega_{ge}(t)$ is the pulse acting between the manifolds, or ultrashort optical pulse, while $\Omega_i(t)$ and $\Omega_f(t)$ are pulses acting within each substructure at the early or late stages of the dynamics; that is, they are infrared pulses.

Then we can set up the functional $\mathcal{D}$,

$$\mathcal{D} = |\langle\psi(0)|U_i(0,\ t_i;\ \Omega_i)\ U_{ge}(t_i,\ t_f;\ \Omega_{ge})\ U_f(t_f,\ T;\ \Omega_f)|\psi_t\rangle|^2 \tag{1}$$

to maximize the transition probability subject to variational changes in the participating fields. Notice that in eq 1 we already constrain the optimization by imposing a sequential operation of the pulses. This constraint is motivated by the different time scales that operate or can operate in the dynamics, as the bandwidths and pulse durations of optical and infrared pulses are typically very different. Without loss of generality we will assume that the initial wave function is the lowest sublevel of the ground state, $|\psi(0)\rangle = |g,1\rangle$. In the following, we will keep $\Omega_{ge}(t)$ as a fixed field, a transform-limited pulse, and analyze the optimization as a function of the "local-in-time" initial and final fields, $\Omega_i(t)$ and $\Omega_f(t)$. Although the functional is always the transition probability, to avoid confusion, we change the notation whenever we make any of the "local" fields equal to zero.

Geometrical Preoptimization: Operating with Ω_i. We will first reduce the scope of the search of the optimal pulses such that $\Omega_f = 0$ and $t_f = T$. Several examples of such control were proposed where an initial (IR) pulse works on the initial state building the necessary coherences before a second pulse moves the population to the excited state.[30−32] Changing the notation of the functional, we call $\mathcal{F} = |\langle\psi_t|U_{ge}(T,t_i;\Omega_{ge})\ U_i(t_i,0;\Omega_i)|\psi(0)\rangle|^2$.

However, instead of explicitly finding the field Ω_i that maximizes $\mathcal{F}$, we will assume (full or partial) controllability within the ground substructure, such that any wave function $|\psi_i\rangle$ that is a superposition of N_i sublevels (a subset of the full set of sublevels of the initial manifold, $N_i \leq N_g$), $|\psi_i\rangle = \sum_j^{N_i} a_j|g,j\rangle$, can be prepared at time t_i.[33,34] Therefore, instead of finding $|\psi_i\rangle = U_i(0,t_i;\Omega_i)\ |g,1\rangle$, we will find $R_i|g,1\rangle = |\psi_i\rangle$ such that $\mathcal{F}$ is maximal as a function of $\Omega_{ge}(t)$, that is kept as a fixed parameter during the optimization. We thus substitute $U_i(t_i,0;\Omega_i)|\psi(0)\rangle$ by $|\psi_i\rangle$ in eq 1. The optimization is purely geometrical, and one can use the Rayleigh−Ritz approach. Restricting $|\psi_i\rangle$ to be normalized (equivalently, R_i to be unitary) by means of the Lagrange multiplier χ_i, the unconstrained functional is $\mathcal{F}' = \mathcal{F} - \chi_i(\langle\psi_i|\psi_i\rangle - 1)$. Formal derivation gives

$$\frac{\partial\mathcal{F}'}{\partial\langle\psi_i|} = U_{ge}(0,\ T;\ \Omega_{ge})|\psi_t\rangle\langle\psi_t|U_{ge}(T,\ 0;\ \Omega_{ge})|\psi_i\rangle - \chi|\psi_i\rangle$$

Upon maximization (i.e., making the derivative equal to zero) we obtain the secular equation,

$$U_{ge}(0,\ T;\ \Omega_{ge})|\psi_t\rangle\langle\psi_t|U_{ge}(T,\ 0;\ \Omega_{ge})|\psi_i\rangle = \chi_i|\psi_i\rangle$$

Or, as a function of the expansion coefficients a_j,

$$\frac{\partial\mathcal{F}'}{\partial a_j^*} = \sum_k (\langle g,\ j|U_{ge}(0,\ T;\ \Omega_{ge})|\psi_t\rangle\langle\psi_t|U_{ge}(T,\ 0;\ \Omega_{ge})|g,\ k\rangle - \chi_i\delta_{jk})a_k = 0$$

(δ_{jk} being the Kronecker delta) leading to the eigenvalue equation

$$\sum_{k=1}^{N_i} F_{jk}a_k = \chi_i a_j \tag{2}$$

where

DOI: 10.1021/acs.jctc.5b00522
J. Chem. Theory Comput. 2015, 11, 4005−4010

$$F_{jk} = \langle g, j|U_{ge}(t_i, T; \Omega_{ge})PU_{ge}(t_i, T; \Omega_{ge})|g, k\rangle \quad (3)$$

and $P = |\psi_t\rangle\langle \psi_t|$ is the projection operator on the target state. The solutions of eq 2 provide the set of eigenvectors that maximize (or minimize) $\mathcal{F}$. In this work we will mostly consider only the eigenvector with maximum eigenvalue, responsible for the largest yield of population transfer. Because we use a geometrical approach, the time t_i is arbitrary and can be relabeled as $t = 0$. On the other hand, quantum optimal control theory (QOCT) or any other dynamic approach could be used to optimize $\Omega_{ge}(t)$, but in this work $\Omega_{ge}(t)$ will be predetermined to favor a particular excitation mechanism. We will use transform-limited (Gaussian) pulses of area[36] $A = \int_0^\infty \Omega_{ge}(t')\, dt'$ and the results of the GO will be parametrized as a function of A.

Identifying $U_{ge}(t_i,T;\Omega_{ge})PU_{ge}(T,t_i;\Omega_{ge})$ as $\rho_t(0)$, one can interpret $\mathcal{F} = \langle\psi_i|\rho_t(0)|\psi_i\rangle$ as an element of the target density matrix propagated to the initial time, which must be maximized. In principle, if there is no constraint in $|\psi_i\rangle$, for pure systems the maximum eigenvalue of $\rho_t(0)$ is always 1. This statement is equivalent to recognizing that the system is fully controllable. However, $|\psi_i\rangle$ is constrained so that only certain superpositions, those involving a subset (or a full set) of the initial manifold, can be prepared. Thus, optimal yields much lower than 1 can be expected, depending on the problem.

One can easily design less-detailed optimization targets. For instance, instead of trying to reach the target state $|\psi_t\rangle$, one can sum the populations of the different sublevels of the final manifold, not requiring excitation of any particular sublevel. This amounts to substituting $\rho_t(T)$ by the target operator

$$P = \rho_t^r(T) = \sum_n^{N_f} |e, n\rangle\langle e, n| \quad (4)$$

Rendering the problem in terms of the density matrices allows one to treat open-system dynamics without changes in the formalism. Only the dynamical equations are different, and instead of the time-dependent Schrödinger equation one needs to solve the corresponding quantum Master equation to obtain ρ_t at initial time. If, in addition, the initial state is not pure, but a density matrix, $\rho_i = \sum_k p_k(0)|g,k\rangle\langle g,k|$, where $p_k(0)$ are the initial populations, then the same formalism can be applied to optimize the action of the initial rotation, R_i, on a single wave function $|g,j\rangle$, typically the one with the largest population.

Geometrical Postoptimization: Operating with Ω_f. In the previous section we maximized the transition probability by acting on the initial state with $\Omega_i(t)$, assuming partial controllability on a set of ground vibrational levels. Now we make $\Omega_i(t) = 0$ and act on the system only within the set of vibrational levels of the excited electronic state by means of $\Omega_f(t)$. Since $\Omega_i(t) = 0$, we can make $t_i = 0$ in eq 1. The restricted functional is now called $\mathcal{G}$. Reorganizing the functional we write

$$\mathcal{G} = \langle\psi_t|U_f(T, t_f; \Omega_f)\, \rho_i(t_f)\, U_f(t_f, T; \Omega_f)|\psi_t\rangle \quad (5)$$

where $\rho_i(t_f) = U_{ge}(t_f0;\Omega_{ge})\ \rho(0)\ U_{ge}(0,t_f;\Omega_{ge})$ is the initial density matrix propagated to t_f. The concept of geometrical postoptimization can then be developed following closely the preoptimization procedure. By substituting the final time-evolution operator by a rotation matrix on the full (or partial) set of sublevels of the final manifold ($N_f \le N_e$), $R_f|\psi_t\rangle = |\psi_f\rangle = \sum_n^{N_f} c_n|e,n\rangle$, and applying the Rayleigh–Ritz method (relabeling the arbitrary t_f as T), we obtain

$$\sum_{n=1}^{N_f} G_{mn}c_n = \chi_f c_m \quad (6)$$

where $G_{mn} = \langle e,m|\rho_i(T)|e,n\rangle$.

For the state-to-state transition, the equations for pre- and postgeometrical optimization are identical. However, the maximum yields, χ_i and χ_f, can differ because the ground and excited substructures may have different features important for the optimization, such as a different number of sublevels that can be reached (that are controllable) or different energy spacings. There is also an important time asymmetry present, because while $\rho_t(T)$ is decided by the controller, $\rho_i(0)$ is given (typically, the ground state).

Double-Time Geometrical Optimization: Operating with Ω_i and Ω_f. We now return to the original functional $\mathcal{D}$ (eq 1) that is maximized with respect to both $|\psi_i\rangle = \sum_j a_j|g,j\rangle$ and $|\psi_f\rangle = \sum_n c_n|e,n\rangle$ and study time-ordered wave function optimizations in the ground and excited manifolds. As was done previously, adopting the geometrical approach implies that no pulses, Ω_i and Ω_f, will be explicitly found. We can therefore regard t_i as $t = 0$ and t_f as $t = T$. Applying the variational method to normalized initial and final optimal wave functions gives the coupled eigenvalue equations ($j \in [1,N_i]$; $m \in [1,N_f]$),

$$\begin{aligned}&\langle g, j|U_{ge}(0, T)|\psi_f\rangle\langle\psi_f|U_{ge}(T, 0)|\psi_i\rangle = \chi\langle g, j|\psi_i\rangle\\ &\langle e, m|U_{ge}(T, 0)|\psi_i\rangle\langle\psi_i|U_{ge}(0, T)|\psi_f\rangle = \chi\langle e, m|\psi_f\rangle\end{aligned} \quad (7)$$

APPLICATIONS

Preparing Quantum Superposition States. As an interesting control problem, we use the GO schemes for preparing particular superposition states in the excited manifold. This is a key step, for instance, in any quantum information device based on molecules.[29] We consider the simplest system, with just two sublevels in each manifold and equal dipoles. The sublevels in each manifold can be degenerate or have some energy splitting ΔE which we take as equal on both manifolds. Since we use Gaussian pulses with bandwidths larger than the energy splitting, the results are not sensitive with respect to small variations among the splitting in the ground and excited states. Therefore, the diagonal elements of the Hamiltonian, H, are $\langle g,1|H|g,1\rangle = \langle e,1|H|e,1\rangle = 0$ and $\langle g,2|H|g,2\rangle = \langle e,2|H|e,2\rangle = \Delta E$, while the only nonzero nondiagonal terms are $\langle e,n|H|g,j\rangle = -\Omega(t)/2$, for $j,n = 1,2$.

We solve the time-dependent Schrödinger equation using a Runge–Kutta method.[35] For each value of the pulse area we solve the dynamics and then apply the different GO schemes, eqs 2, 6, and 7, which provide the optimal initial (and final) states, that is, the eigenvectors with maximum eigenvalue. Figure 1 shows the probability of finding the system in the superposition state $|\varphi_{e,\pm}\rangle = (|e,1\rangle \pm |e,2\rangle)/\sqrt{2}$ at final time, starting from the preoptimized initial state, $|\psi_i\rangle$, as a function of the pulse area. In Figure 1a we show the results when the sublevels are degenerate, $\Delta E = 0$. In this case, for every pulse area the optimized state is always $|\psi_i\rangle = |\varphi_{g,+}\rangle = (|g,1\rangle + |g,2\rangle)/\sqrt{2}$. We have recently shown analytically[27] that this wave function leads to $|\varphi_{e,+}\rangle$ at half odd multiples of π by parallel transfer. $|\varphi_{e,-}\rangle$ is, on the other hand, a dark state, and the maximum population in $|e,1\rangle$ and $|e,2\rangle$ never exceeds 0.5. The same result is obtained using the postoptimization scheme. State-selective population transfer can be achieved by the double-time geometrical optimization procedure, following the

DOI: 10.1021/acs.jctc.5b00522
J. Chem. Theory Comput. 2015, 11, 4005–4010

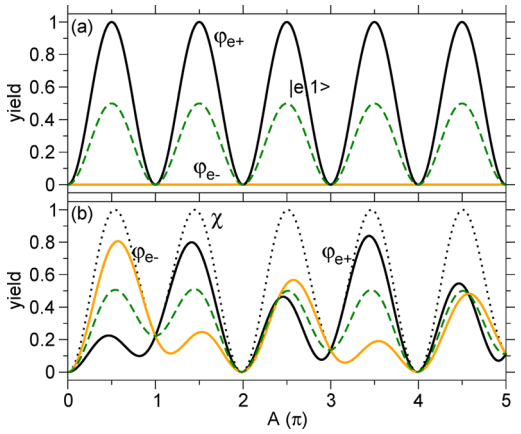

Figure 1. Yields of population transfer to certain states at final time as a function of pulse area, A, in a system with two states with (a) two degenerate sublevels and (b) two sublevels with energy splitting ΔE = 0.4. Using preoptimization, we show the probability of reaching states $|\varphi_{e,+}\rangle$ (solid line), $|\varphi_{e,-}\rangle$ (red line), and $|e,j\rangle$ (dashed line), which coincides with the probability of postoptimization of any state in the final manifold, and the overall probability in the final manifold (dotted lines), which coincides with the probability χ of reaching any state in the final manifold by double-time optimization. In panel a these lines overlap the probability in $|\varphi_{e,+}\rangle$.

protocol $|g,1\rangle \overset{R_i}{\Rightarrow} |\varphi_{g,+}\rangle \overset{\Omega_{ge}}{\Rightarrow} -i|\varphi_{e,+}\rangle \overset{R_f}{\Rightarrow} |\psi_t\rangle$ that guarantees full population transfer after each Rabi oscillation, in agreement with the pulse area theorem.[36]

In Figure 1b the energy splitting in both manifolds is $\Delta E = 0.4 < \Delta\omega_{ge} = 4 \ln 2$ (where $\Delta\omega_{ge}$ is the bandwidth of the pulse, with scaled width, $\tau = 1$). The preoptimization solution is similar to the previous one, but now the final probability of exciting $|\varphi_{e,+}\rangle$ is smaller, whereas $|\varphi_{e,-}\rangle$ is no longer dark. Depending on the pulse area, one superposition state is favored over the other. By postoptimization one cannot obtain yields much larger than 0.5. Except for very specific target states, pre- and postoptimization tend to give similar results, especially when N_i and N_f increase. Although full population transfer to specific superposition states is no longer possible, full Rabi-flipping to the excited manifold, corresponding to the preoptimization of a less-refined target, can still be achieved at particular pulse areas, and the same result is obtained using the double-time optimization procedure.

Efficiency Thresholds of Population Transfer. We now evaluate the different efficiency thresholds that are typically achieved for the yields of selective population transfer using the different GO procedures previously outlined. In this work $\Omega_{ge}(t)$ is limited to broadband transform-limited pulses. Then a worse-case scenario[27] is observed for degenerate substructures, that is, systems where all sublevels in both the ground and excited manifolds are degenerate. We will assume that all couplings between sublevels of the ground and excited manifolds are equal and one, such that $\langle e,n|H|g,j\rangle = -\Omega_{ge}(t)/2$, $\forall\, n \in N_e$, and $j \in N_g$. This defines the Hamiltonian of the so-called degenerate symmetrical structure, the dynamics of which is analytical under transform-limited pulses,[27,37]

$$U_{nj}(\infty) = \langle e,\, n|U(\Omega_{ge})|g,\, j\rangle = -\frac{i}{\sqrt{N_e N_g}} \sin\left(\sqrt{N_g N_e}\, A/2\right) \tag{8}$$

Since all of the matrix elements of the time-evolution operator are identical in eq 3, and equivalently for G_{mn}, we find that

$$F_{jk} = G_{mn} = \frac{1}{N_g N_e} \sin^2\left(\sqrt{N_g N_e}\, A/2\right) = P_{if}$$

where P_{if} is the state-to-state transition probability (when no GO scheme is applied). The eigenvalue equation for the preoptimization (eq 2) of any Hamiltonian eigenstate $|e,k\rangle$ of the excited manifold becomes $P_{if} \sum_j^{N_i} a_j = \chi_i a_k$, $\forall\, k \in N_i$ with maximum eigenvalue

$$\chi_i = N_i P_{if} \tag{9}$$

and eigenvector $|\psi_i\rangle = \sum_j^{N_i} |g,j\rangle/\sqrt{N_i}$, which gives parallel transfer while all of the remaining eigenvectors have zero eigenvalue, corresponding to dynamics of laser-induced transparency.[38,39] This solution minimizes the detrimental role of the Stark-shifts. The maximum possible yield for populating an excited Hamiltonian eigenstate is $\chi_i = 1/N_e$, accessible at particular pulse areas only when $N_f = N_e$ and hence limited by the number of sublevels in the excited manifold. On the other hand, because of parallel transfer, $|\psi_i\rangle$ leads to $|\varphi_{e,+}\rangle = \sum_j^{N_e} |e,j\rangle/\sqrt{N_e}$, and the pulse area theorem assures full population transfer to a particular superposition state for certain pulse areas, as shown in Figure 1.

Consider now a less-refined target such as the yield of the overall manifold-to-manifold transition given by eq 4. Then $F_{ij} = N_e P_{if}$ and therefore

$$\chi_i^r = N_i N_e P_{if} \tag{10}$$

yielding full population inversion between the manifolds ($\chi_i^r = 1$) when there is full controllability on the manifold of ground sublevels. For postoptimization, again there is a single eigenvalue different from zero which gives a maximum yield of

$$\chi_f = N_f P_{if} \tag{11}$$

for which $|\psi_f\rangle = \sum_n^{N_f} |e,n\rangle/\sqrt{N_f}$. The absolute maximum yield, $\chi_f = 1/N_i$, is now limited by the number of levels in the ground manifold.

Finally, in solving eqs 7 by substituting $|\psi_i\rangle$ and $|\psi_f\rangle$ for the parallel transfer solutions, one obtains

$$\chi = N_i N_f P_{if} = \frac{N_i}{N_g}\frac{N_f}{N_e} \sin^2\left(\sqrt{N_g N_e}\, A/2\right) \tag{12}$$

The results of Figure 1a provide a particular example of these estimates. The probability of reaching $|\varphi_{e,+}\rangle$ (oscillating from 0 to 1) coincides with the yield of nonselective excitation by preoptimization and with the yield of state-selective excitation (of any pure state in the excited manifold) by means of double-time optimization. On the other hand, the probability of reaching $|e,1\rangle$ and $|e,2\rangle$ oscillates up to 0.5 and is the same as the yield by postoptimization. Although the bounds given by eqs 9−12 are only exact for the degenerate symmetrical structure, they give lower bounds for a much larger set of systems whenever $\Delta E \ll \Delta\omega_{ge}$, as shown by numerical evidence. For comparison, Figure 2 shows the average maximum population transfer (the average of the first five peaks of the Rabi oscillations) for systems with increasing number of sublevels and different energy spacings. The yields are always bounded from below by the analytical thresholds

DOI: 10.1021/acs.jctc.5b00522
J. Chem. Theory Comput. 2015, 11, 4005−4010

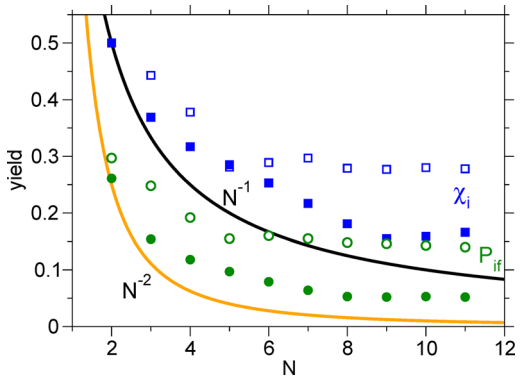

Figure 2. Average maximum yield for population transfer to $|e,1\rangle$ without optimization (P_{if}, circles) and with preoptimization (χ_i, squares) for systems with an increasing number of levels $N = N_g = N_e$ and different energy splittings, $\Delta E = 0.2$ (filled symbols) and 0.4 (open symbols). The average is performed with respect to the first five maxima in the Rabi oscillations. For reference, the black and orange lines show the analytical results for degenerate systems, $\chi_i = N^{-1}$ and $P_{if} = N^{-2}$. The double-time geometrical optimization (not shown) always gives average maximum yields $\chi = 1$.

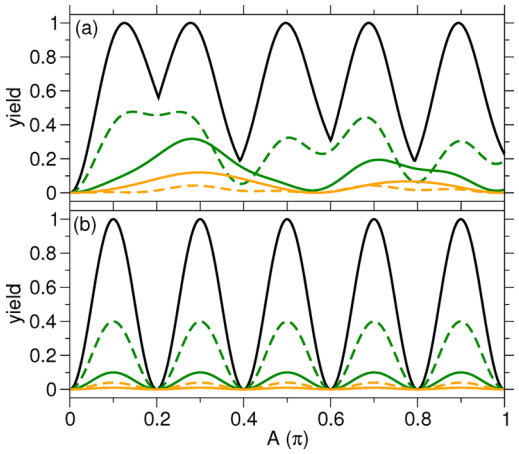

Figure 3. Yields of population transfer as a function of the pulse area, A, for the transition to weakly coupled states in a system with four sublevels in each manifold, with (a) $\Delta E = 0$ and (b) $\Delta E = 0.4$. The black lines show the result of double-time optimization, χ. The green lines show the probability to reach states $|e,4\rangle$ (dashed line) and $|e,1\rangle$ (solid line) with preoptimization. Orange lines give the results without optimization.

found for the degenerate system. Initially, the yields decay approximately as N^{-1} and N^{-2} for χ_i and P_{if}. However, for a given bandwidth, there is a maximum effective number of levels that participate (that can be excited by the pulse) in the dynamics, roughly $N_{max}\Delta E \sim 1$. If N_i increases beyond N_{max}, the remaining levels are not *active* and the yields do not further decay, as Figure 2 shows.

Selective Excitation of Weakly Coupled States. Finally, we analyze state-selective excitation in systems with different transition dipoles or Franck−Condon (FC) factors. The goal here is to see under what conditions it is possible to achieve population inversion to weakly coupled excited states.

As an example, we consider a Hamiltonian with equally spaced vibrational levels in the ground and excited electronic states, $\langle g,n|H|g,n\rangle = \langle e,n|H|e,n\rangle = (n-1)\Delta E$ and couplings that increase with the vibrational excitation (approximately as in two displaced harmonic oscillators), $\langle e,n|H|g,j\rangle = -\sqrt{jn}\,\Omega_{ge}(t)/2$, $\forall\, n \in N_e$ and $j \in N_g$. Clearly, without optimization, for broadband pulse excitation the transition from $|g,1\rangle$ to $|e,4\rangle$ is weak and $|e,1\rangle$ is almost dark. In addition, in the presence of energy splittings (and assuming ω_{ge} is on resonance for the $|g,1\rangle \rightarrow |e,1\rangle$ transition), $|e,4\rangle$ can be hardly excited due to the energy detuning. Figure 3 shows the final probabilities as a function of the pulse area for a system with $N_e = N_g = 4$ and $\Delta E = 0$ or 0.4 with no GO and using preoptimization and double-time optimization. In the degenerate system the FC factors alone determine the outcome of the dynamics, so that the double-time optimization is completely necessary for state-selective excitation. For $\Delta E = 0.4$, a simple preoptimization solution (to move the population from $|g,1\rangle \rightarrow |\psi_i\rangle \approx |g,4\rangle$, where the coupling is larger) is enough to yield almost 50% population transfer at particular pulse areas. However, one needs both pre- and postoptimization to obtain larger yields.

CONCLUSIONS

In summary, we have proposed a general method of quantum control via geometrical optimization particularly suited to understand properties of the control of population transfer in molecules or other quantum structures. The method relies on factoring the time-evolution operator and substituting each local part by a rotation in its proper Hilbert subspace. We have applied the scheme to study state-selective broadband population transfer between sublevels that belong to two different manifolds. By engineering the initial state before the application of the pulse, it is possible to transfer all of the population between the manifolds. However, only very specific superposition states can be prepared with high fidelity, as the yields typically decay with the number of levels in the excited or initial manifolds. Full state-selective population transfer, in particular to dark or weakly coupled states, requires both engineering the initial state and having full control over the excited manifold at final times. However, it is not necessary to control the dynamics within the manifolds at all times.

The use of GO as a function of different laser parameters, as the pulse area, allows one to better understand the limitations that the parameters impose on the dynamics and suggests physically motivated ways of lifting those limitations, as reflected on the quantum landscapes. The methods used here are not meant as an alternative to QOCT, since both approaches aim at different types of solutions. Whereas in QOCT an optimal field is found, in our approach the field is implicit: only the optimized wave function is found by the variational approach. On the other hand, while in QOCT it is difficult to impose hard constraints, typically yielding poor optimization results, the GO gives the optimal wave function given the desired structural constraints by a fast matrix diagonalization. Both methods can be used in a complementary way. One can use GO to identify the main vibrational levels that should participate in the dynamics in order to achieve high yields and then apply QOCT to find the pulse that prepares such wave function or uses such pathways.[25] One could use this approach with several intermediate steps. In addition, one can use the GO together with the QOCT approach, lifting the constraints on the optical pulse such that instead of using it as a fixed parameter, the pulse is optimized via QOCT. In this work we have only shown a few limited examples of the power of the geometrical optimization approach, but the same ideas can be applied to more complex structures, requiring more fields, or to

DOI: 10.1021/acs.jctc.5b00522
J. Chem. Theory Comput. 2015, 11, 4005−4010

other interesting molecular processes, for instance photoassociation reactions or quantum information processing.

AUTHOR INFORMATION

Corresponding Author

*E-mail: isola@quim.ucm.es.

Funding

This work was supported by the NRF Grant funded by the Korean government (Grant 2007-0056343), the International cooperation program (Grant NRF-2013K2A1A2054518), the Basic Science Research program (Grant NRF-2013R1A1A2061898), the EDISON project (Grant 2012M3C1A6035358), and the MICINN Project CTQ2012-36184.

Notes

The authors declare no competing financial interest.

ACKNOWLEDGMENTS

I.R.S. acknowledges R. Pardo for many fruitful conversations and the Korean Brain Pool Program for support.

REFERENCES

(1) Rice, S. A.; Zhao, M. *Optical Control of Molecular Dynamics*; John Wiley & Sons: New York, 2000.
(2) Shapiro, M.; Brumer, P. *Quantum Control of Molecular Processes*, 2nd Revised and Enlarged ed.; Wiley-VCH: Weinheim, Germany, 2012.
(3) D'Alessandro, D. *Introduction to Quantum Control and Dynamics*; Chapman & Hall: Boca Raton, FL, USA, 2008.
(4) Brif, C.; Chakrabarti, R.; Rabitz, H. *Adv. Chem. Phys.* **2011**, *148*, 1−76.
(5) Nielsen, M. A.; Chuang, I. L. *Quantum Computation and Quantum Information*; Cambridge University Press: Cambridge, U.K., 2000.
(6) Peirce, A. P.; Dahleh, M. A.; Rabitz, H. *Phys. Rev. A: At., Mol., Opt. Phys.* **1988**, *37*, 4950−4965.
(7) Tannor, D. J.; Rice, S. A. *J. Chem. Phys.* **1985**, *83*, 5013−5018.
(8) Kosloff, R.; Rice, S. A.; Gaspard, P.; Tersigni, S.; Tannor, D. *Chem. Phys.* **1989**, *139*, 201−220.
(9) Werschnik, J.; Gross, E. K. U. *J. Phys. B: At., Mol. Opt. Phys.* **2007**, *40*, R175−R211.
(10) Huang, G. M.; Tarn, T. J.; Clark, J. W. *J. Math. Phys.* **1983**, *24*, 2608−2618.
(11) Schirmer, S. G.; Fu, H.; Solomon, A. *Phys. Rev. A: At., Mol., Opt. Phys.* **2001**, *63*, 063410.
(12) Rabitz, H. A.; Hsieh, M. M.; Rosenthal, C. M. *Science* **2004**, *303*, 1998−2001.
(13) Rabitz, H.; Hsieh, M.; Rosenthal, C. *Phys. Rev. A: At., Mol., Opt. Phys.* **2005**, *72*, 052337.
(14) Chakrabarti, R.; Rabitz, H. *Int. Rev. Phys. Chem.* **2007**, *26*, 671−735.
(15) Shi, S.; Rabitz, H. *J. Chem. Phys.* **1990**, *92*, 2927−2937.
(16) Sola, I. R.; Muñoz-Sanz, R.; Santamaria, J. *J. Phys. Chem. A* **1998**, *102*, 4321−4327.
(17) Mancal, T.; May, V. *Chem. Phys. Lett.* **2002**, *362*, 407−413.
(18) Doria, P.; Calarco, T.; Montangero, S. *Phys. Rev. Lett.* **2011**, *106*, 190501.
(19) Caneva, T.; Calarco, T.; Montangero, S. *Phys. Rev. A: At., Mol., Opt. Phys.* **2011**, *84*, 022326.
(20) Hornung, T.; Motzkus, M.; de Vivie-Riedle, R. *Phys. Rev. A: At., Mol., Opt. Phys.* **2002**, *65*, 021403(R).
(21) Gollub, C.; Kowalewski, M.; de Vivie-Riedle, R. *Phys. Rev. Lett.* **2008**, *101*, 073002.
(22) Palao, J. P.; Reich, D. M.; Koch, C. P. *Phys. Rev. A: At., Mol., Opt. Phys.* **2013**, *88*, 053409.
(23) Reich, D. M.; Palao, J. P.; Koch, C. P. *J. Mod. Opt.* **2014**, *61*, 822−827.
(24) Shi, S.; Rabitz, H. *J. Chem. Phys.* **1990**, *92*, 364−376.
(25) Jakubetz, W.; Kades, E.; Manz, J. *J. Phys. Chem.* **1993**, *97*, 12609−12619.
(26) Sola, I. R.; Malinovsky, V. S.; Tannor, D. J. *Phys. Rev. A: At., Mol., Opt. Phys.* **1999**, *60*, 3081−3090.
(27) Chang, B. Y.; Shin, S.; Sola, I. R. *J. Phys. Chem. Lett.* **2015**, *6*, 1724−1728.
(28) Szabo, A.; Ostlund, N. S. *Modern Quantum Chemistry: Introduction to Advanced Electronic Structure Theory*; Dover Publications: Mineola, NY, USA, 1996.
(29) de Vivie-Riedle, R.; Troppmann, U. *Chem. Rev.* **2007**, *107*, 5082−5100.
(30) Amstrup, B.; Henriksen, N. E. *J. Chem. Phys.* **1992**, *97*, 8285−8295.
(31) Meyer, S.; Engel, V. *J. Phys. Chem. A* **1997**, *101*, 7749−7753.
(32) Elghobashi, N.; González, L. *Phys. Chem. Chem. Phys.* **2004**, *6*, 4071−4073.
(33) Turinici, G.; Rabitz, H. *Chem. Phys.* **2001**, *267*, 1−9.
(34) Turinici, G.; Rabitz, H. *J. Phys. A: Math. Gen.* **2003**, *36*, 2565−2576.
(35) Press, W. H.; Teukolsky, S. A.; Vetterling, W. T.; Flannery, B. P. Integration of Ordinary Differential Equations. *Numerical Recipes in Fortran 90. The Art of Parallel Scientific Computing*, Vol. 2; Cambridge University Press: New York, 1996; pp 704−708.
(36) Shore, B. W. Two-state coherent excitation. *Manipulating Quantum Structures Using Laser Pulses*; Cambridge University Press: Cambridge, U.K., 2011; pp 97−136.
(37) Rangelov, A. A.; Vitanov, N. V.; Shore, B. W. *Phys. Rev. A: At., Mol., Opt. Phys.* **2006**, *74*, 053402.
(38) Boller, K. J.; Imamoglu, A.; Harris, S. E. *Phys. Rev. Lett.* **1991**, *66*, 2593−2596.
(39) Eberly, J. H.; Pons, M. L.; Haq, H. R. *Phys. Rev. Lett.* **1994**, *72*, 56−59.

DOI: 10.1021/acs.jctc.5b00522
J. Chem. Theory Comput. 2015, 11, 4005−4010